ISSN 2070-2051, Protection of Metals and Physical Chemistry of Surfaces, 2025, Vol. 61, No. 2, pp. 301–318. © Pleiades Publishing, Ltd., 2025.

NANOSCALE AND NANOSTRUCTURED MATERIALS AND COATINGS

Efficiency Enhancement of GaN/InN-Based Solar Cells through Doping with Si, Zn, Ag Elements: A Physico-Chemical Study of Nanosurface by First-Principles Calculation

Fatemeh Mollaamin*

Department of Biomedical Engineering, Faculty of Engineering and Architecture, Kastamonu University, Kastamonu, Turkey
**e-mail: fmollaamin@kastamonu.edu.tr*

Received January 27, 2025; revised February 17, 2025; accepted March 3, 2025

Abstract—As applied materials for storage energy in solar cells, hetero clusters of GaN, InN, GaInN, GaInSiN, GaInZnN, GaInAgN can attract considerable attention in materials science. A comprehensive investigation on energy grabbing by GaN, InN, GaInN, GaInSiN, GaInZnN, GaInAgN was carried out including using DFT computations at the CAM-B3LYP-D3/6-311+G(d,p) level of theory. Electromagnetic and thermodynamic properties of GaN, InN, GaInN, GaInSiN, GaInZnN, GaInAgN hetero clusters have been evaluated. The hypothesis of the energy adsorption phenomenon was confirmed by density distributions of CDD, PDOS, and ESP for GaN, InN, GaInN, GaInSiN, GaInZnN, GaInAgN hetero clusters. The two hetero clusters of GaInZnN and GaInAgN with the fluctuations of In, Ga, N and transition metals of Zn, Ag have indicated the same sensitivity graph of electric potential via charge distribution with $R^2_{Zn/Ag-GaInN} = 0.9998$. Therefore, it can be considered that zinc and silver atoms in the functionalized GaInZnN and GaInAgN may have more effective sensitivity for admitting the electrons in the status of energy adsorption mechanism. Furthermore, GaInAgN is potentially advantageous for certain high-frequency applications requiring solar cells for energy storage. The advantages of silver over indium gallium nitride include its higher electron and hole mobility, allowing silver doping devices to operate at higher frequencies than silicon and zinc doping devices. As a matter of fact, it can be observed that doped hetero clusters of GaInZnN and GaInAgN might ameliorate the capability of GaInN in solar cells for energy storage.

Keywords: solar cells, energy storage, GaN, InN, GaInN, GaInSiN, GaInZnN, GaInAgN, hetero cluster, DFT

DOI: 10.1134/S2070205125700212

1. INTRODUCTION

Gallium nitride (GaN) is a very hard material with wide bandgap applied in a variety of technologies, including optoelectronic, high-power electronics and light-emitting diodes, partly due to its favorable thermal properties [1, 2]. The nitrides of group III in periodic table have low sensitivity to ionizing radiation which make them appropriate materials for solar cell arrays for satellites. Therefore, space applications could also benefit as devices have shown stability in high radiation environments. Because GaN transistors can operate at much higher temperatures and work at much higher voltages than gallium arsenide (GaAs) transistors, they make ideal power amplifiers at microwave frequencies. In addition, GaN offers promising characteristics for THz devices. Due to high power density and voltage breakdown limits GaN is also emerging as a promising candidate for 5G cellular base station applications [3, 4].

GaN with a high crystalline quality can be obtained by depositing a buffer layer at low temperatures [5]. Such high-quality GaN led to the discovery of *p*-type GaN [6], *p*–*n* junction blue/UV-LEDs [6] and room-temperature stimulated emission [7]. This has led to the commercialization of high-performance blue LEDs and long-lifetime violet laser diodes, and to the development of nitride-based devices such as UV detectors and high-speed field-effect transistors [8]. GaN-based metal–oxide–semiconductor field-effect transistor (MOSFET) and metal–semiconductor field-effect transistor (MESFET) transistors also offer advantages including lower loss in high power electronics, especially in automotive and electric car applications [9]. The U.S. Army Research Laboratory (ARL) provided the first measurement of the high field electron velocity in GaN in 1999 [10]. Scientists at ARL experimentally obtained a peak steady-state velocity of 1.9×10^7 cm/s, with a transit time of 2.5 ps, attained at an electric field of 225 kV/cm. With this information, the electron mobility was calculated, thus providing data for the design of GaN devices.

The ternary semiconductor of Indium gallium nitride (InGaN) as solar cells is remarkable owing to

the adjustable direct band gap energy of InGaN veiling the total solar spectrum arraying from 0.7 to 3.4 eV [11, 12], as well as preferable photovoltaic specifics of InGaN consisting of vast absorption coefficients [13] and high carrier dynamism. Furthermore, great fixity and excellent radiation persistence of InGaN alloys permit function of InGaN-based instruments in the uttermost situations such as space and geocentric usages [11, 14]. The solar cells of InGaN were constructed with low indium amounts of the InGaN alloy compounds [15–17] which conduces to an enhancement in the band gap energy of InGaN and then eventuates in the absorption of shorter wavelengths of solar radiation. Therefore, to find out InGaN solar cells with high yield, the In amount in the InGaN active layer of these solar cells should be enhanced to compensate a large part of the solar spectrum. Recently, it has been suggested the application of dual nanogratings of Si and other organic solar cells which are mostly in direct contact with the active area of the solar cells [18–24]. Moreover, the researchers fabricated transition metal zinc doped InGaN nanorods arrays by radio-frequency plasma-assisted molecular beam epitaxy. The doping obviously reduces indium atoms composition, the aggregation of In–In and induces the deep energy level. This greatly decreases the defects and improves the valence band potential of InGaN nanorods [25].

Recently, researchers have proposed an InGaN/GaN *p–i–n* thin-film solar cell which includes a dual nanograting compound: silver nanogratings on the back of the solar cell and GaN-NGs on the front. FDTD simulation parameters have exhibited that the dual NG compound connects the eventual sunlight to the plasmonic and photonic styles, so enhancing the absorption of the solar cell in a wide spectral span. It is perceived that the solar cells possessing the double nanograting structures have a considerable increment in light absorption compared with cells having either no nanogratings or having only the front nanogratings or only the back nanogratings [26].

In this paper, we propose a feasible ternary semiconductor of the indium gallium nitride solar cell which is doped with silicon, zinc or silver. We carried out molecular modelling considering the geometrical parameters of doping atoms on the surface of GaInN through the absorption status and current charge density of the solar cells was studied. Moreover, the effect of a relative chemical shift between GaInN and doped hetero clusters of the solar cell was also investigated.

2. EXPERIMENTAL

Silicon-, zinc-, or silver-doped GaInN solar cells were calculated within the framework of first-principles calculation based on density functional theory (DFT) (Fig. 1). The rigid potential energy surface using density functional theory [27–40] was performed due to Gaussian 16 revision C.01 program package [41] and GaussView 6.1 [42]. The coordination input for energy storage on the solar cells has applied 6-311+G(d,p) and EPR-3 basis sets.

Figure 1 has shown the process of energy storage on hetero clusters of GaN, InN, GaInN, GaInSiN, GaInZnN, and GaInAgN which is modified to enlarge the absorption in the active zone. Further, we optimized the structural parameters of nanocages of GaN, InN, a ternary semiconductor of GaInN solar cell which is doped with silicon, zinc or silver towards formation of hetero clusters of GaInSiN, GaInZnN, GaInAgN for obtaining the greatest short current aggregate in these solar cell structures.

3. RESULTS AND DISCUSSION

The data in this work has evaluated the efficiency of hetero clusters of GaN, InN, GaInN, GaInSiN, GaInZnN, GaInAgN hetero clusters for storage energy in solar cells.

3.1. Charge Density Differences

The amounts of charge density differences (CDD) are measured by considering isolated atoms or noninteracting ones. The mentioned approximation can be the lightest to use because the superposition value may be received from the primary status of the self-consistency cycle in the code that carries out the density functional theory (Figs. 2a–2f) [43].

In Fig. 2a, the atoms of N(10), N(12), N(14), N(16), N(17) from GaN have shown the fluctuation around –9 to 4.5 Bohr. The atoms of N(10), N(14), N(16), N(17) from InN have indicated the fluctuation around –9 to 5 Bohr (Fig. 2b). In Fig. 2c, the atoms of N(10), N(14) extracted from ternary hereto-cluster of GaInN have exhibited the fluctuation around –9 to 5.5 Bohr. Then, the two doped hereto-clusters of GaInSiN (Fig. 2d) and GaInZnN (Fig. 2e) with active atoms of N(10), N(14), N(16), N(17) have been oscillated around –9 to 2.5 Bohr. However, in doped hereto-cluster of GaInAgN, except for atoms of N(10), N(14), N(16), N(17), the Ag (5) has been considered as a fluctuated atom around –9 to 3 Bohr (Fig. 2f).

3.2. Partial Density of State

Squirming the molecular orbital data owing to gaussian graphs of unit altitude and entire width at half maximum (FWHM) of 0.3 eV by GaussSum 3.0.2 [44] have computed partial density of state (PDOS). Figures 3a–3f) shows the partial density of state (PDOS) of GaN, InN, GaInN, GaInSiN, GaInZnN, GaInAgN hetero clusters. The appearance of the energy states (*d*-orbital) of Si, Zn, Ag doped on GaN, InN, GaInN, GaInSiN, GaInZnN, GaInAgN hetero clusters induces the reactivity of the system. It is clear from the figure that after atom doping, there is a significant contribution of *p*-orbitals of N and Si atoms in the

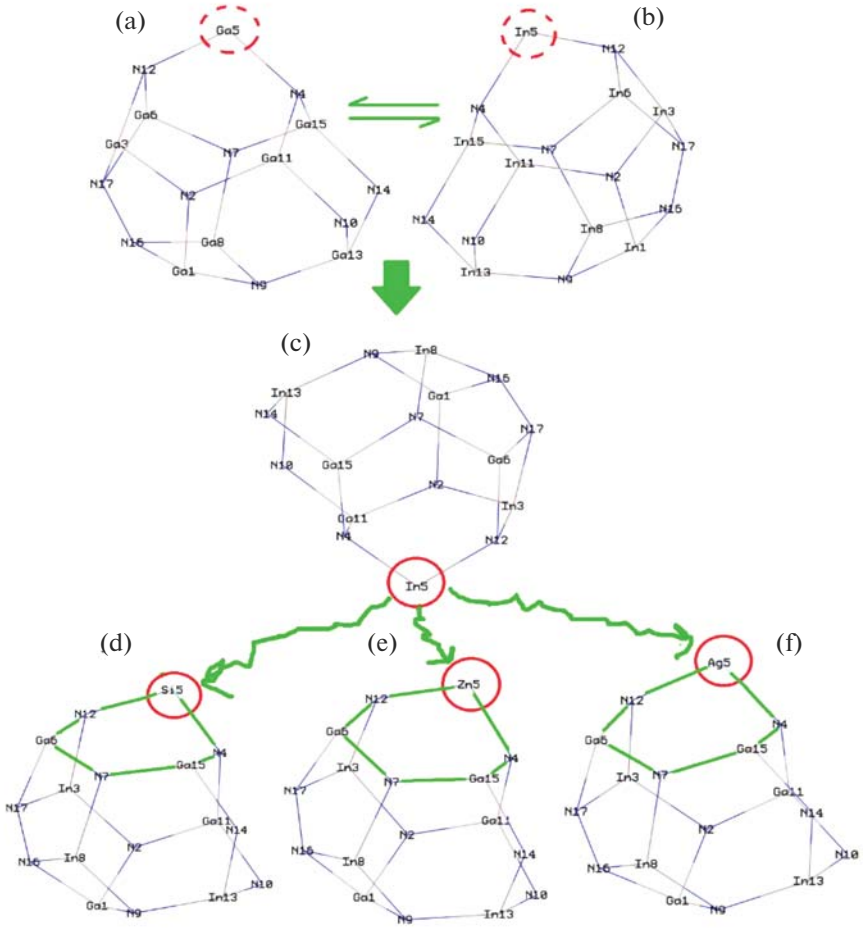

Fig. 1. Application of hetero clusters of (a) GaN, (b) InN, (c) GaInN, (d) GaInSiN, (e) GaInZnN, and (f) GaInAgN for energy storage in solar cells using CAM-B3LYP-D3/6-311+G(d,p) calculation.

unoccupied level of GaN, InN, GaInN, GaInSiN, GaInZnN, GaInAgN hetero clusters. Therefore, the curve of partial PDOS has described the *p* states of N and Si atoms and *d*-orbitals of Ga, In, Zn, Ag atoms in GaN, InN, GaInN, GaInSiN, GaInZnN, GaInAgN overcome due to the conduction band (Figs. 3a–3f).

It has been shown that GaN, InN, GaInN, GaInSiN, GaInZnN, GaInAgN hetero clusters through atom doping have the most contribution at the middle of the conduction band between −5 to −10 eV, while contribution of nitrogen, silicon, zinc and silver states are enlarged and similar together, and doping atoms depicts interfacial electronic of the GaN, InN, GaInN, GaInSiN, GaInZnN, GaInAgN hetero clusters. GaN, InN, GaInN hetero clusters have indicated sharp peaks for N atoms in Figs. 3a, 3b, 3c), respectively. GaInSiN has exhibited strong peaks for N and Si atoms close to each other (Fig. 3d). The sharp N graph near Zn atoms in GaInZnN has been indicated (Fig. 2e). Furthermore, GaInAgN has indicated sharp peaks for N atoms close to Ag atom in Fig. 2f.

3.3. Molecular Electrostatic Potential

Molecular electrostatic potential (ESP) measures the electrostatic interaction between a unit point charge placed at "*r*" and the system of interest. A positive (negative) value implies that the current position is dominated by nuclear (electronic) charges. ESP has been widely used for prediction of nucleophilic and electrophilic sites for a long time. It is also valuable in studying hydrogen bonds, halogen bonds, molecular recognitions and the intermolecular interaction of aromatics [45].

$$V_{\text{tot}}(r) = V_{\text{nuc}}(r) + V_{\text{ele}}(r) = \sum_A \frac{Z_A}{|r - R_A|} - \int \frac{\rho(r')}{|r - r'|} dr', \quad (1)$$

where Z_A is nuclear charge, if pseudopotential is used, then Z_A is the number of explicitly expressed electrons. Notice that evaluating ESP is much more time-consuming than evaluating other functions. Also note that ESP in Multiwfn is evaluated exactly by nuclear attractive integrals rather than using approximate methods (such as multipole expansion, numerical

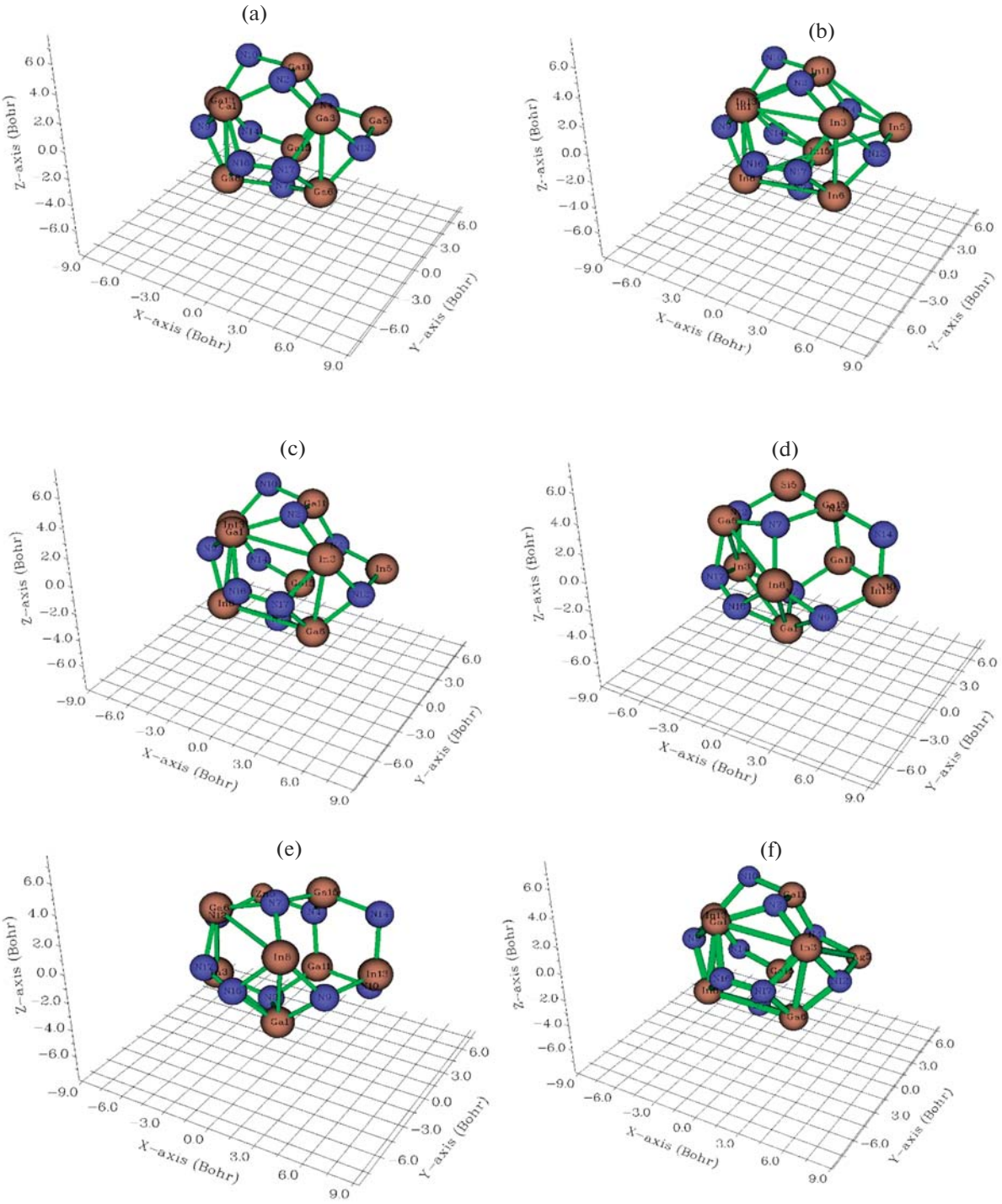

Fig. 2. CDD graphs for hetero clusters of (a) GaN, (b) InN, (c) GaInN, (d) GaInSiN, (e) GaInZnN, and (f) GaInAgN.

Poisson equation), hence you may find the results generated by Multiwfn [46, 47] are somewhat different from those outputted by other quantum chemistry codes. In order to speed up ESP evaluation, Multiwfn ignores some integrals that have little contributions. The threshold for ignoring is controlled by "esppre-cutoff" in settings.ini, enlarging this parameter results in more accurate ESP value, but also brings more computational cost. The ESP evaluated under default value is accurate enough in general cases.

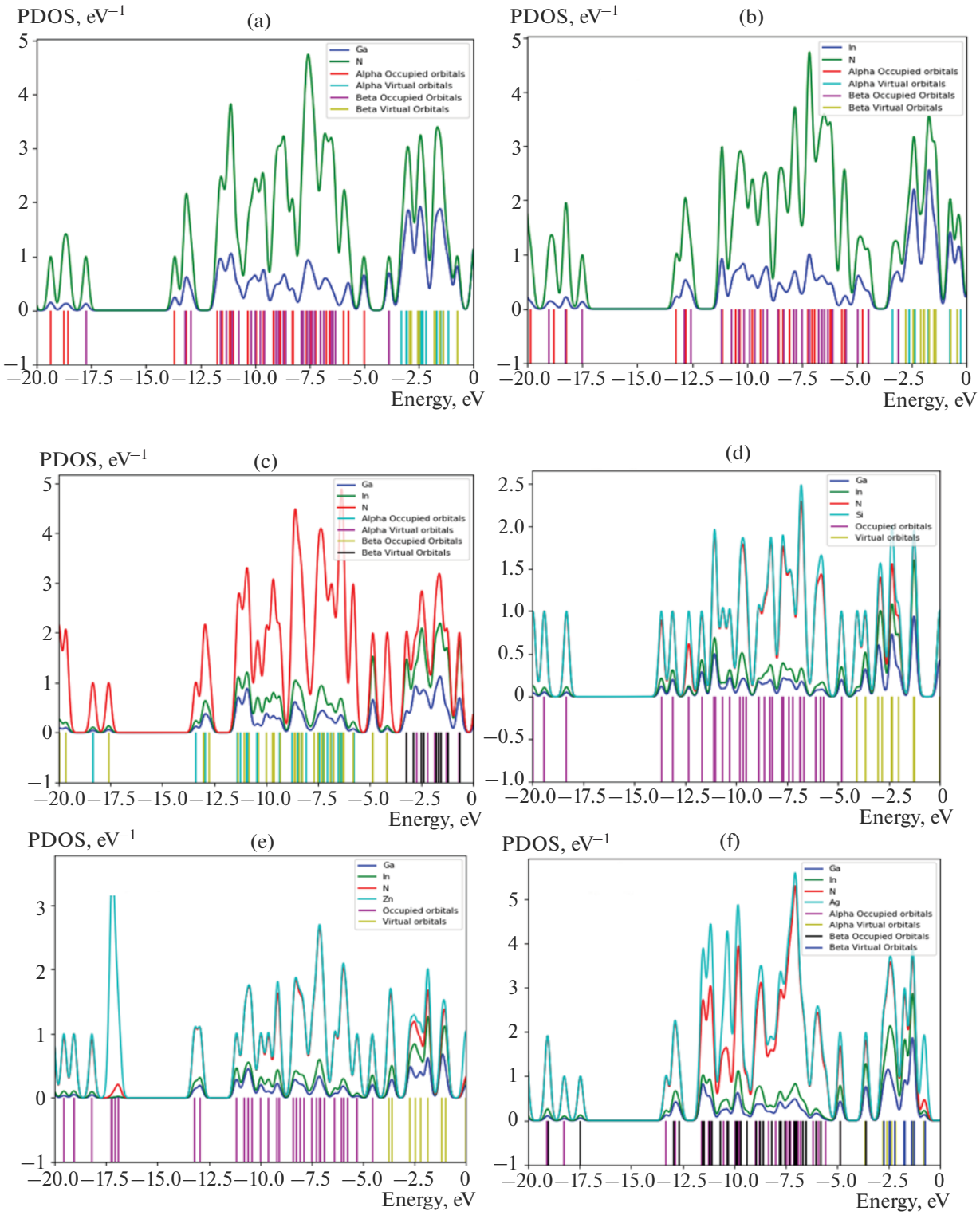

Fig. 3. PDOS graphs of hetero clusters include (a) GaN, (b) InN, (c) GaInN, (d) GaInSiN, (e) GaInZnN, and (f) GaInAgN.

The compounds of GaN, InN, GaInN, GaInSiN, GaInZnN, and GaInAgN can be defined by ESP graphs owing to exploring their delocalization/localization characterizations of electrons and chemical bonds (Figs. 4a–4f).

The counter map of ESP for GaN and InN has shown the electron delocalization of these two hetero-clusters based on labeling atoms of N(4), Ga(5), Ga(15) for GaN(Fig. 4a) and N(4), In (5), In(15) for InN (Fig. 4b), respectively. Then, the formation of

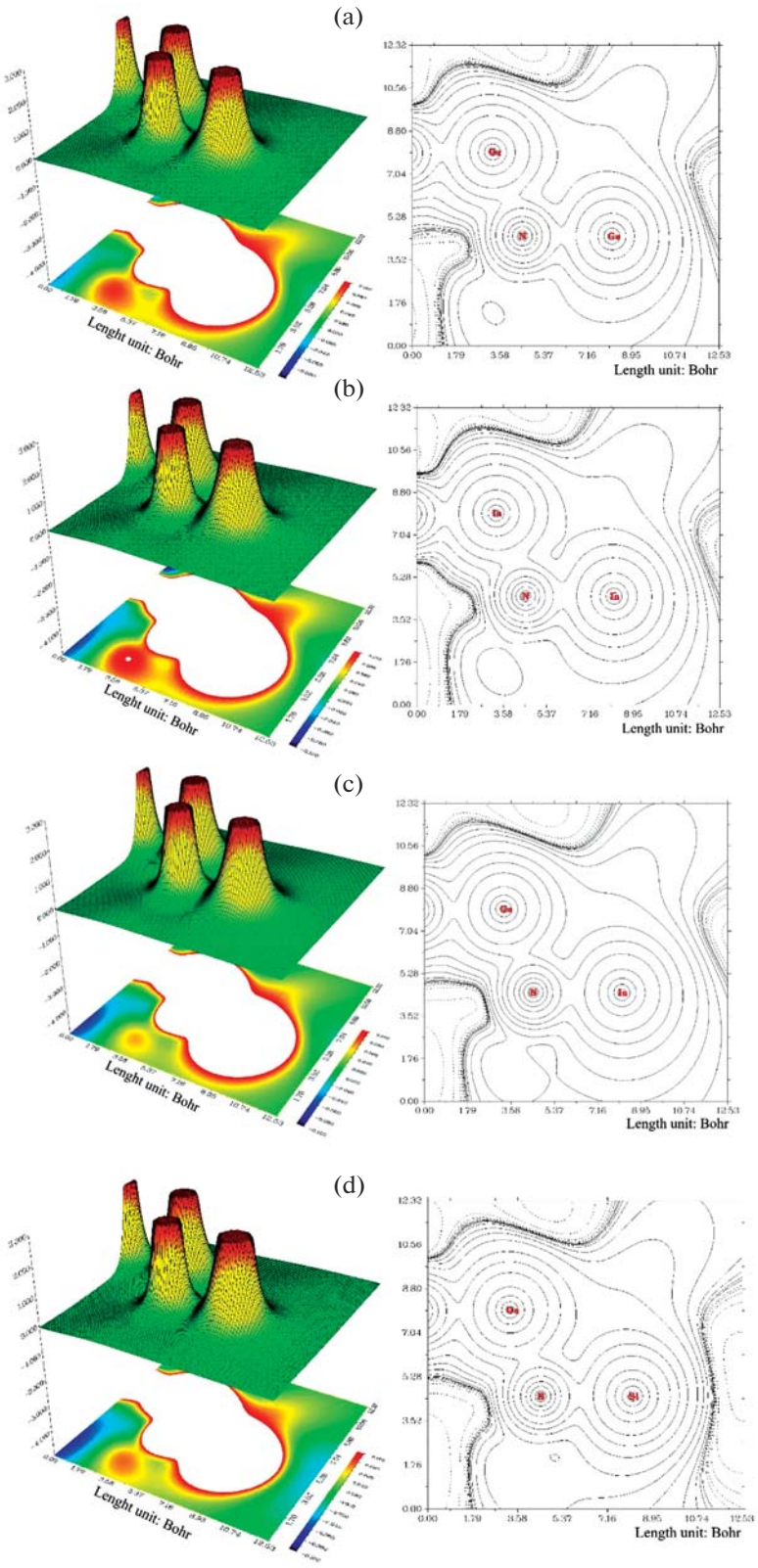

Fig. 4. The graphs of ESP for hetero clusters include (a) GaN, (b) InN, (c) GaInN, (d) GaInSiN, (e) GaInZnN, and (f) GaInAgN. (Counter line map on the right and shaded surface map with projection in the left).

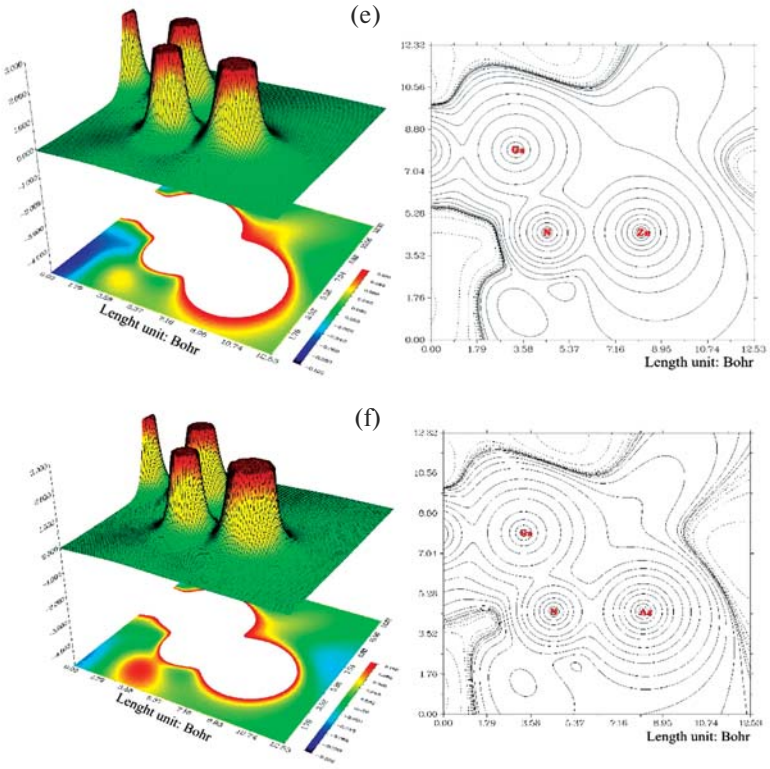

Fig. 4. (Contd.)

ternary alloy of GaInN indicates an isosurface map of electron delocalization due to labeling atoms of N(4), In(5), Ga(15) (Fig. 4c). A vaster jointed area engaged by an isosurface map for Si, Zn, Ag doping GaInN towards formation of hetero clusters of GaInSiN (Fig. 4d), GaInZnN (Fig. 4e) and GaInAgN (Fig. 4f) due to labeling atoms of N(4), Si/Zn/Ag (5), Ga(15), respectively. A narrower connected area occupied by an isosurface map means that electron delocalization is relatively difficult. However, the large counter map of ESP for GaInAgN, GaInZnN, GaInSiN hetero clusters can confirm that doping Ag, Zn, Si nanoparticles on the surface, respectively, increases the efficiency of ternary solar cell of GaInN for energy storage.

Besides, the changes of charge density analysis have illustrated that $In_3Ga_4N_9$ has shown the Bader charge of −1.131 C, and after doping with silicon, zinc and silver has indicated the Bader charge of −1.172, −1.171, and −1.159 C for GaInSiN, GaInZnN, GaInAgN, respectively, that describes the tensity value of these hetero clusters for energy storage.

3.4. Theory of Nuclear Quadrupole Resonance (NQR)

The NQR frequencies have been measured for GaN, InN nanocages, ternary alloy of $In_3Ga_4N_9$ and doped hetero clusters of GaInSiN, GaInZnN, GaInAgN (Table1). The NQR method is related to the multipole expansion in Cartesian coordinates as the Eq. (2) [48, 49]:

$$V(r) = V(0) + \left[\left(\frac{\partial V}{\partial x_i}\right|_0 x_i\right)\Bigg] + \frac{1}{2}\left[\left(\frac{\partial^2 V}{\partial x_i x_j}\right|_0 x_i x_j\right)\Bigg] + \ldots \quad (2)$$

After that, a simplification on the Eq. (2), there are only the second derivatives related to the identical variable for the potential energy [48, 49]:

$$\begin{aligned} U &= -\frac{1}{2}\int_{\mathscr{D}} d^3 r \rho_r \left[\left(\frac{\partial^2 V}{\partial x_i^2}\right|_0 x_i^2\right)\Bigg] \\ &= -\frac{1}{2}\int_{\mathscr{D}} d^3 r \rho_r \left[\left(\frac{\partial E_i}{\partial x_i}\right|_0 x_i^2\right)\Bigg] \\ &= -\frac{1}{2}\left(\frac{\partial E_i}{\partial x_i}\right|_0 \int_{\mathscr{D}} d^3 r \left[\rho(r) x_i^2\right]. \end{aligned} \quad (3)$$

There are two parameters which must be gotten from NQR experiments: the quadrupole coupling constant, χ, and asymmetry parameter of the EFG tensor η:

$$\chi = e^2 Q q_{zz}/h, \quad (4)$$

$$\eta = q_{xx} - q_{yy}/q_{zz}, \quad (5)$$

Table 1. The electric potential (E_p, a.u.) and Bader charge (Q, C) through NQR calculation for hetero clusters of GaN, InN, GaInN, GaInSiN, GaInZnN, and GaInAgN

GaN			InN			GaInN		
atom	Q	E_p	atom	Q	E_p	atom	Q	E_p
Ga(1)	1.0254	−1.2452	In(1)	1.0892	−1.1272	Ga(1)	0.9707	−1.2502
N(2)	−1.0773	−18.4020	N(2)	−1.1142	−18.4464	N(2)	−1.0703	−18.4221
Ga(3)	1.0235	−1.2349	In(3)	1.0608	−1.1218	In(3)	1.0927	−1.1250
N(4)	−1.0919	−18.4117	N(4)	−1.0816	−18.4647	N(4)	−1.0491	−18.4426
Ga(5)	0.7423	−1.2568	In(5)	0.7515	−1.1445	In(5)	0.8477	−1.1369
Ga(6)	1.0234	−1.2349	In(6)	1.0434	−1.1267	Ga(6)	0.9434	−1.2497
N(7)	−1.0772	−18.4020	N(7)	−1.0888	−18.4528	N(7)	−1.0733	−18.4211
Ga(8)	1.0250	−1.2453	In(8)	1.1043	−1.1287	In(8)	1.1306	−1.1245
N(9)	−1.0668	−18.4133	N(9)	−1.0859	−18.4638	N(9)	−1.0911	−18.4432
N(10)	−0.7024	−18.4144	N(10)	−0.7607	−18.4624	N(10)	−0.7137	−18.4101
Ga(11)	1.0584	−1.2403	In(11)	1.1060	−1.1353	Ga(11)	0.9581	−1.2549
N(12)	−1.0605	−18.4073	N(12)	−1.0766	−18.4554	N(12)	−1.0483	−18.4420
Ga(13)	0.9727	−1.2496	In(13)	1.0075	−1.1543	In(13)	1.0453	−1.1333
N(14)	−0.7022	−18.4144	N(14)	−0.8211	−18.4702	N(14)	−0.7305	−18.4126
Ga(15)	1.0582	−1.2403	In(15)	1.0648	−1.1406	Ga(15)	0.9633	−1.2549
N(16)	−0.5733	−18.3576	N(16)	−0.6007	−18.3934	N(16)	−0.5936	−18.3766
N(17)	−0.5774	−18.3543	N(17)	−0.5978	−18.3932	N(17)	−0.5820	−18.3784
GaInSiN			GaInZnN			GaInAgN		
atom	Q	E_p	atom	Q	E_p	atom	Q	E_p
Ga(1)	1.0110	−1.2324	Ga(1)	0.9829	−1.2458	Ga(1)	1.0034	−1.2384
N(2)	−1.0887	−18.4073	N(2)	−1.0717	−18.4279	N(2)	−1.1010	−18.4179
In(3)	1.1339	−1.1107	In(3)	1.0865	−1.1302	In(3)	1.0758	−1.1370
N(4)	−1.1043	−18.4149	N(4)	−1.0547	−18.4375	N(4)	−0.9911	−18.4072
Si(5)	0.7457	−1.9019	Zn(5)	0.8092	−16.2483	Ag(5)	0.4398	−17.8675
Ga(6)	0.9634	−1.2391	Ga(6)	0.9440	−1.2530	Ga(6)	0.9398	−1.2642
N(7)	−1.0730	−18.4143	N(7)	−1.0933	−18.4192	N(7)	−1.1047	−18.4192
In(8)	1.1720	−1.1102	In(8)	1.1708	−1.1155	In(8)	1.1591	−1.1137
N(9)	−1.0737	−18.4330	N(9)	−1.0672	−18.4410	N(9)	−1.1027	−18.4306
N(10)	−0.7574	−18.4233	N(10)	−0.7365	−18.4326	N(10)	−0.7263	−18.4256
Ga(11)	1.0198	−1.24269	Ga(11)	0.9908	−1.2663	Ga(11)	1.0670	−1.2426
N(12)	−1.0932	−18.4110	N(12)	−1.0493	−18.4336	N(12)	−0.9160	−18.4344
In(13)	1.0539	−1.1362	In(13)	1.0236	−1.1476	In(13)	1.0872	−1.1200
N(14)	−0.7532	−18.4207	N(14)	−0.7761	−18.4369	N(14)	−0.7336	−18.4235
Ga(15)	1.0250	−1.2475	Ga(15)	0.9928	−1.2601	Ga(15)	1.0679	−1.2427
N(16)	−0.6046	−18.3630	N(16)	−0.5865	−18.3635	N(16)	−0.6089	−18.3774
N(17)	−0.5766	−18.3600	N(17)	−0.5654	−18.3663	N(17)	−0.5558	−18.3870

where q_{ii} are ingredients of the EFG tensor at the quadrupole nucleus determined in the EFG principal axes system, Q is the nuclear quadrupole moment, e is the proton charge and h is the Planck's constant [50, 51].

In this research work, the electric potential as the quantity of work energy through carrying over the electric charge from one position to another position in the essence of electric field has been evaluated for GaN, InN nanocages, GaInN ternary alloy and doped hetero clusters of Si–GaInN, GaInZnN, GaInAgN (Table1).

In Fig. 5a, the atoms of N(10), N(12), N(14), N(16), N(17) from GaN have shown the fluctuation in the range of –1.5 to 1 C with average electric potential about –18 a.u. The atoms of N(10), N(14), N(16), N(17) from InN have indicated the fluctuation –1.5 to 1 C with average electric potential about –19 a.u (Fig. 5b). In Fig. 5c, the atoms of N(10), N(14) extracted from ternary hereto cluster of GaInN have exhibited the fluctuation in the range of –1.5 to 1 C with average electric potential about –20 a.u. Then, the Si-doped hereto-cluster of GaInSiN (Fig. 5d) with active atoms of N(10), N(14), N(16), N(17) has been oscillated in the range of –1.5 to 1 C with average electric potential about –20 a.u. However, in two doped hereto-clusters of GaInZnN (Fig. 5e) and GaInAgN (Fig. 5f) the atoms of N(10), N(14), N(14), N(16), N(17) have been considered as fluctuated atoms between –1.5 to 1 C with average electric potential about –23 a.u. In fact, by doping transition metals of Zn and Ag to GaInN, the electric potential extracted from NQR calculations grows. Therefore, it can be proposed that doped alloys of GaInSiN, GaInZnN, and GaInAgN might augment the ability of GaInN in solar cells for energy storage.

It was observed the behavior of Ga and N atoms in GaN (Fig. 5a) and In and N atoms in InN (Fig. 5b) with vast sensitivity based on relation coefficient of $R^2_{GaN} = 0.9994$ and $R^2_{InN} = 0.9990$; however, ternary alloy of GaInN has shown the behavior of In, Ge and N atoms with high sensitivity due to relation coefficient of $R^2_{GaInN} = 0.9994$ (Fig. 5c). In Fig. 5d, hetero-cluster of GaInSiN exhibited the behavior of Si-doped GaInN with high sensitivity of $R^2_{Si-In_4Ga_4N_9} = 0.9992$. The two hetero clusters of GaInZnN and GaInAgN with the fluctuations of In, Ga, N and transition metals of Zn, Ag have indicated the same sensitivity graph of electric potential via charge distribution with $R^2_{Zn/Ag-In_4Ga_4N_9} = 0.9998$. Therefore, it can be considered that zinc and silver atoms in the functionalized GaInZnN and GaInAgN may have more effective sensitivity for admitting the electrons in the status of energy adsorption mechanism.

3.5. Nuclear Magnetic Resonance Spectra

NMR spectra of GaN, InN, GaInN, GaInSiN, GaInZnN, and GaInAgN hetero clusters as the potential molecules for energy storage can unravel the efficiency of these complexes in solar cells. From the DFT calculations, it has been attained the chemical shielding (CS) tensors in the principal axes system to estimate the isotropic chemical-shielding (CSI) and anisotropic chemical-shielding (CSA) [52]:

$$\sigma_{iso} = (\sigma_{11} + \sigma_{22} + \sigma_{33})/3; \quad (6)$$

$$\sigma_{aniso} = \sigma_{33} - (\sigma_{22} + \sigma_{11})/2. \quad (7)$$

The NMR data of isotropic (σ_{iso}) and anisotropic shielding tensors (σ_{aniso}) of GaN, InN nanocages, ternary alloy of GaInN and doped hetero clusters of GaInSiN, GaInZnN, GaInAgN have been computed by Gaussian 16 revision C.01 program package [41] and been shown in Table 2.

In Table 2, NMR data has reported the notable amounts for GaN, InN, GaInN, GaInSiN, GaInZnN, and GaInAgN hetero clusters. The notable fragile signal intensity close to the parallel edge of the nanocluster sample might be owing to indium or gallium binding induced non-spherical distribution of GaN and InN, nanocages and GaInN hetero cluster. Figures 6a–6f indicated a similar desire of shielding for indium or gallium; however, a notable deviation stands from doping atoms of silicon, zinc and silver as electron acceptors on the surface of GaInN hetero-cluster.

The remarkable enhancement in the chemical shift anisotropy spans for nanocages of GaN (Fig. 6a) and InN (Fig. 6b) is near N(10), N(14), N(16), and N(17). The yield of electromagnetic shifting can be directed by nitrogen atoms of N(10) and N(14) extracted from ternary hereto-cluster of GaInN (Fig. 6c). Figure 6d has shown that the intensity for energy storage can be enhanced in GaInSiN due to oscillating chemical shielding in N(10), N(14), N(16), N(17) atoms. The atoms of N(10), N(14), N(14), N(16), N(17) have indicated the fluctuation in chemical shielding for GaInZnN (Fig. 6e) and GaInAgN (Fig. 6f). So, it can be observed that doped hetero clusters of GaInSiN, GaInZnN, and GaInAgN might ameliorate the capability of GaInN in solar cells for energy storage.

3.6. Insight of Infrared Spectroscopy and Thermochemistry

The infrared spectroscopy (IR) has been performed for GaN, InN nanocages, ternary alloy of GaInN and doped hetero clusters of GaInSiN, GaInZnN, GaInAgN (Figs. 7a–7f). Therefore, it has been simulated to the several clusters containing GaN (Fig. 7a), InN (Fig. 7b), GaInN (Fig. 7c), GaInSiN (Fig. 7d), GaInZnN (Fig. 7e), and GaInAgN (Fig. 7f).

The frequency values through the IR curves between 100–1200 cm^{-1} have been achieved for GaN

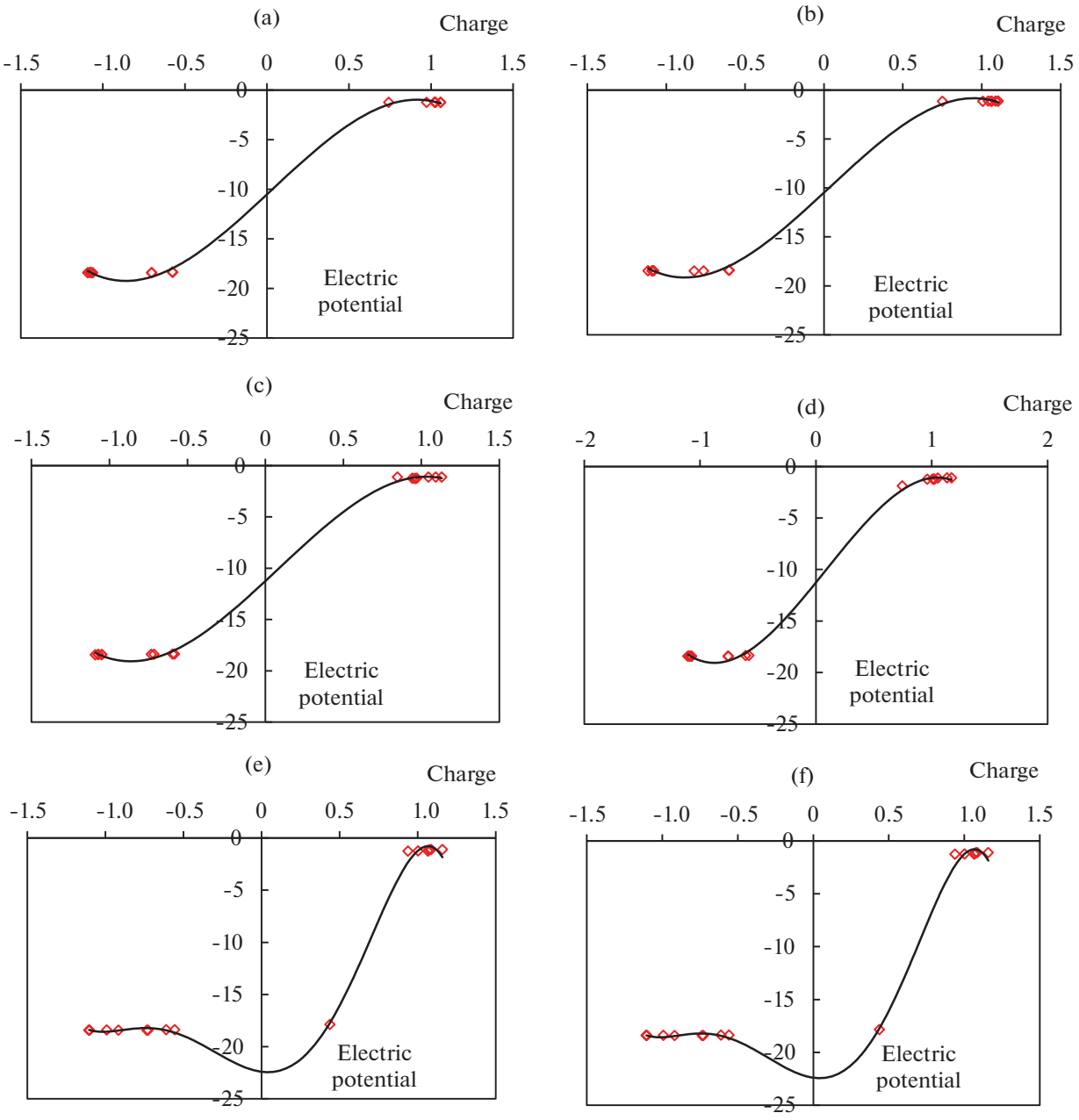

Fig. 5. Electric potential (a.u.) versus Bader charge (C) through NQR calculation for hetero clusters of (a) GaN, (b) InN, (c) GaInN, (d) GaInSiN, (e) GaInZnN, and (f) GaInAgN.

with several sharp peaks around 391.27, 420.84, 451.72, 581.93, 624.62, 686.54, and 692.45 cm^{-1} (Fig. 7a). Figure 7b has shown the frequency range between 100–1200 cm^{-1} for InN with sharp peaks around 356.43, 385.93, 409.88, 416.57, 493.70, and 749.78 cm^{-1}. Figure 7c has indicated the fluctuation of frequency between 100–1200 cm^{-1} for GaInN with sharp peaks around 386.14, 388.65, 450.05, 464.72, and 844.38 cm^{-1}. The graph of Fig. 7d has been observed in the frequency range between 200–1100 cm^{-1} for GaInSiN with several sharp peaks around 372.66, 377.37, 425.97, 643.15, 658.78, 814.28, and 1001.62 cm^{-1}. Figure 7e has shown the frequency range between 100–1100 cm^{-1} for GaInZnN with sharp peaks around 344.39, 363.95, 374.21, 391.72, 443.55, 660.86, 689.18, 808.93, and 953.51 cm^{-1}. Fur-

Table 2. Data of NMR shielding tensors (ppm) for selected atoms of hetero clusters containing GaN, InN, GaInN, GaInSiN, GaInZnN, and GaInAgN

GaN			InN			GaInN		
atom	σ_{iso}	σ_{aniso}	atom	σ_{iso}	σ_{aniso}	atom	σ_{iso}	σ_{aniso}
Ga(1)	10.0053	7.2179	In(1)	8.9768	9.3388	Ga(1)	6.3534	14.8126
N(2)	65.1694	155.1736	N(2)	108.1694	231.6895	N(2)	49.3767	1236.9875
Ga(3)	7.4014	5.3803	In(3)	9.3930	8.0909	In(3)	10.0551	6.2745
N(4)	0.8995	198.1397	N(4)	122.4153	219.9847	N(4)	407.8588	737.1718
Ga(5)	2.2013	8.5732	In(5)	10.6746	5.9066	In(5)	10.7712	14.1226
Ga(6)	7.4064	5.4070	In(6)	9.7751	4.0554	Ga(6)	7.1354	11.6367
N(7)	65.4722	154.4676	N(7)	60.3992	239.6405	N(7)	158.3084	1243.0308
Ga(8)	10.0093	7.1774	In(8)	8.9983	10.0737	In(8)	11.0774	11.3480
N(9)	87.2703	157.7915	N(9)	27.4571	274.2831	N(9)	271.9379	914.8715
N(10)	962.1326	1264.6912	N(10)	1103.6930	1399.6850	N(10)	2443.1570	30749.2042
Ga(11)	1.9610	11.1990	In(11)	1.2753	13.2851	Ga(11)	0.6521	159.3123
N(12)	181.8466	386.9313	N(12)	17.2322	108.5181	N(12)	21.7219	371.0508
Ga(13)	1.5411	20.6497	In(13)	0.5443	14.8402	In(13)	103.6089	276.0002
N(14)	961.9570	1263.8589	N(14)	428.7716	783.3209	N(14)	2062.3661	25680.5093
Ga(15)	1.9811	11.2049	In(15)	6.3166	7.9155	Ga(15)	27.5315	130.6120
N(16)	146.7792	296.0469	N(16)	189.5344	411.9799	N(16)	149.9103	453.1744
N(17)	185.7863	358.9644	N(17)	212.8650	452.6256	N(17)	193.3085	401.4953
GaInSiN			GaInZnN			GaInAgN		
atom	σ_{iso}	σ_{aniso}	atom	σ_{iso}	σ_{aniso}	atom	σ_{iso}	σ_{aniso}
Ga(1)	22.4538	78.4944	Ga(1)	9.3316	37.4650	Ga(1)	4.2860	11.2048
N(2)	90.5435	2353.7072	N(2)	229.6976	1052.3678	N(2)	90.8706	242.4258
In(3)	0.5915	36.8612	In(3)	14.5568	13.2011	In(3)	9.1190	4.9193
N(4)	352.5209	741.5237	N(4)	44.3468	780.9040	N(4)	206.1374	466.9775
Si(5)	34.5396	70.5497	Zn(5)	95.9880	131.0803	Ag(5)	131.6129	127.7348
Ga(6)	14.6808	34.8610	Ga(6)	6.5185	11.6063	Ga(6)	6.3971	4.7338
N(7)	36.1844	1582.1437	N(7)	67.5580	506.3021	N(7)	101.4922	225.8792
In(8)	6.4452	31.5713	In(8)	15.8840	24.8787	In(8)	6.8944	10.5657
N(9)	66.7389	1817.1573	N(9)	499.2453	1720.5050	N(9)	8.7336	387.1125
N(10)	21230.9779	62643.4034	N(10)	9100.0648	20128.3772	N(10)	1002.2681	1666.7390
Ga(11)	53.3020	480.0935	Ga(11)	1.2677	182.4448	Ga(11)	3.1143	16.4254
N(12)	22.8449	554.1679	N(12)	143.7794	889.3983	N(12)	185.6084	661.7365
In(13)	236.7296	423.8107	In(13)	67.1945	124.2693	In(13)	5.0613	22.9514
N(14)	5858.9106	55100.5620	N(14)	2466.4255	15963.0699	N(14)	1016.9550	1694.9169
Ga(15)	36.7467	410.7079	Ga(15)	17.2887	118.6204	Ga(15)	3.7978	15.5883
N(16)	84.8309	3132.3787	N(16)	1537.4363	5335.5418	N(16)	106.3362	303.3121
N(17)	632.7758	5076.1741	N(17	687.2490	4281.8851	N(17)	224.9163	360.9659

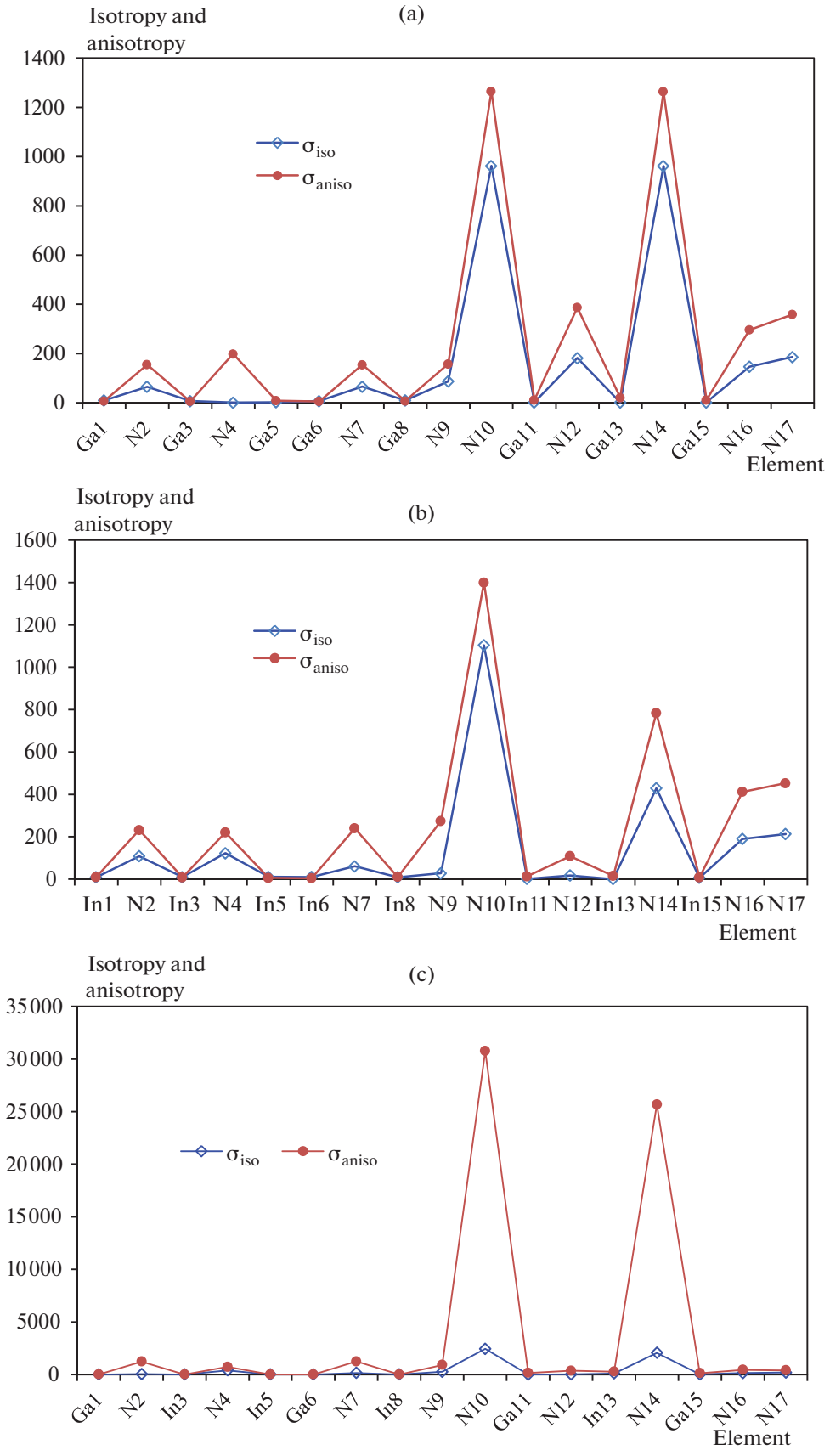

Fig. 6. The NMR spectra for hetero clusters of (a) GaN, (b) InN, (c) GaInN, (d) GaInSiN, (e) GaInZnN, and (f) GaInAgN.

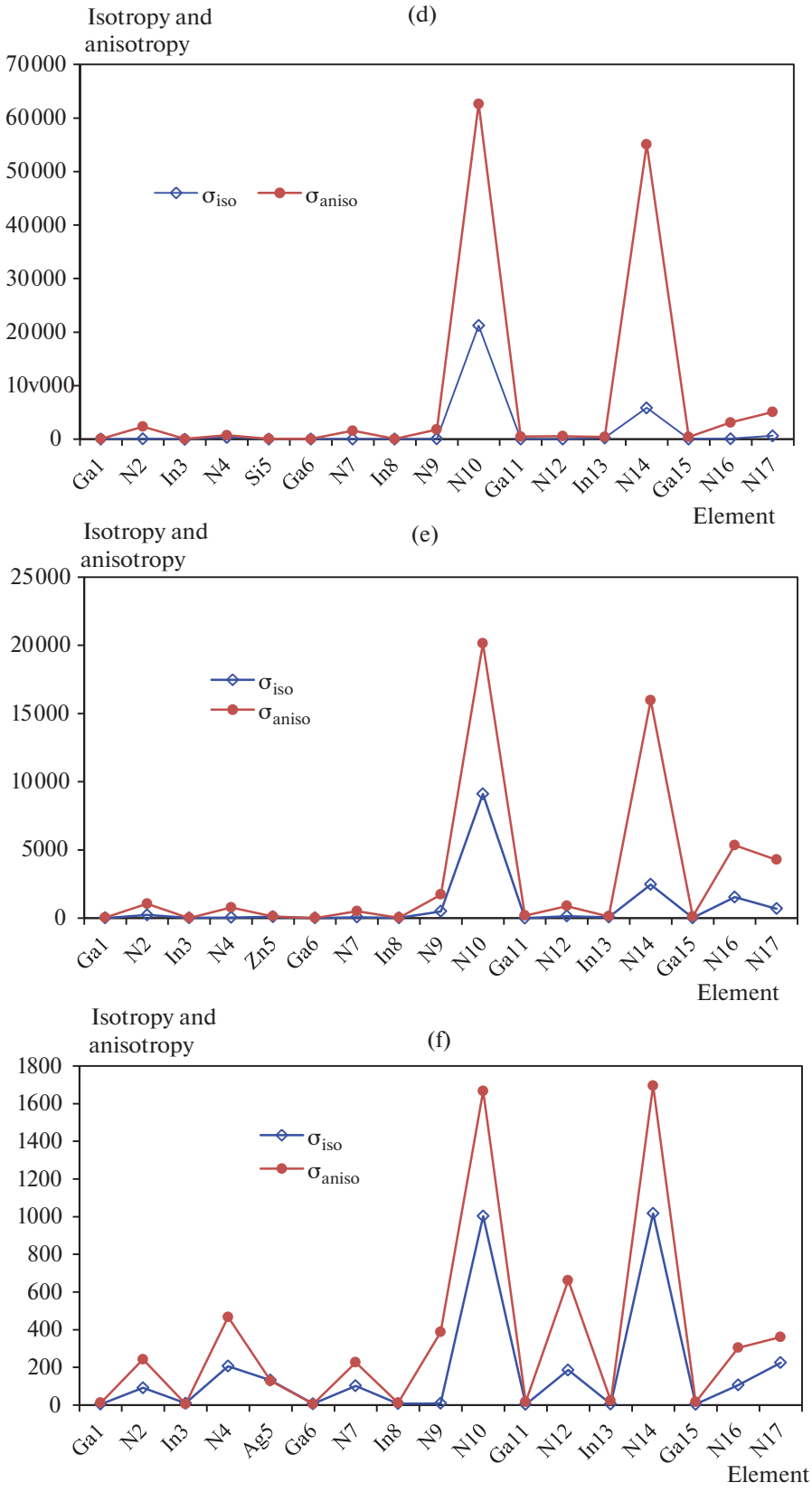
(d)
Isotropy and anisotropy
70000
60000
50000
40000
30000
20000
10v000
0
σiso
σaniso
Ga1 N2 In3 N4 Si5 Ga6 N7 In8 N9 N10 Ga11 N12 In13 N14 Ga15 N16 N17
Element
(e)
Isotropy and anisotropy
25000
20000
15000
10000
5000
0
σiso
σaniso
Ga1 N2 In3 N4 Zn5 Ga6 N7 In8 N9 N10 Ga11 N12 In13 N14 Ga15 N16 N17
Element
(f)
Isotropy and anisotropy
1800
1600
1400
1200
1000
800
600
400
200
0
σiso
σaniso
Ga1 N2 In3 N4 Ag5 Ga6 N7 In8 N9 N10 Ga11 N12 In13 N14 Ga15 N16 N17
Element

Fig. 6. (Contd.)

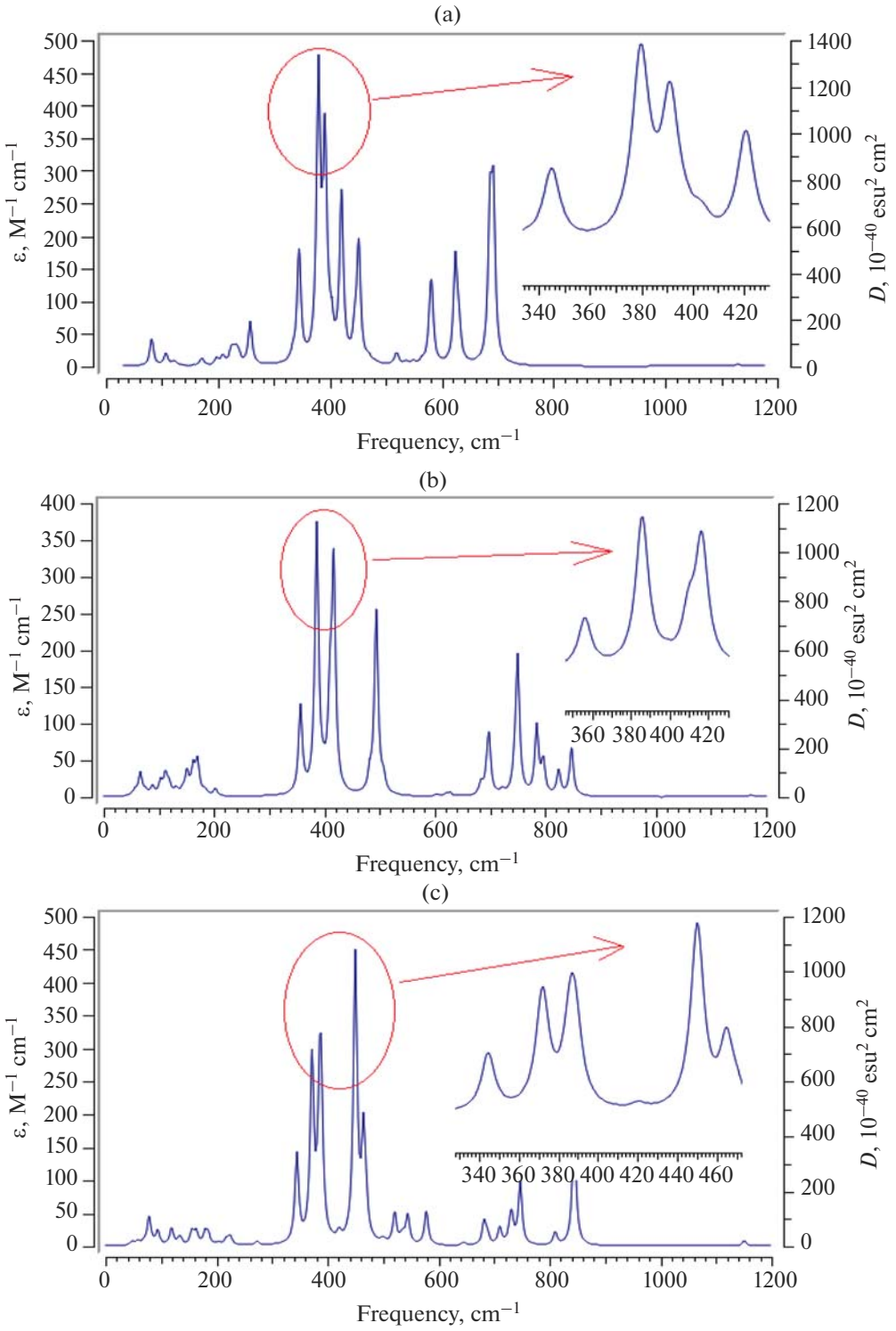

Fig. 7. The frequency (cm^{-1}) changes through the IR spectra for hetero clusters of (a) GaN, (b) InN, (c) GaInN, (d) GaInSiN, (e) GaInZnN, and (f) GaInAgN.

thermore, the graph of Fig. 7f has been observed in the frequency range between 100–1200 cm^{-1} for GaInAgN with several sharp peaks around 364.05, 392.08, 421.72, 720.67, 749.85, and 841.15 cm^{-1}.

Energy storage with hetero clusters has described that the frame of the overcoming cluster is related to GaInAgN in the high amounts of frequency. This property makes GaInAgN potentially advantageous

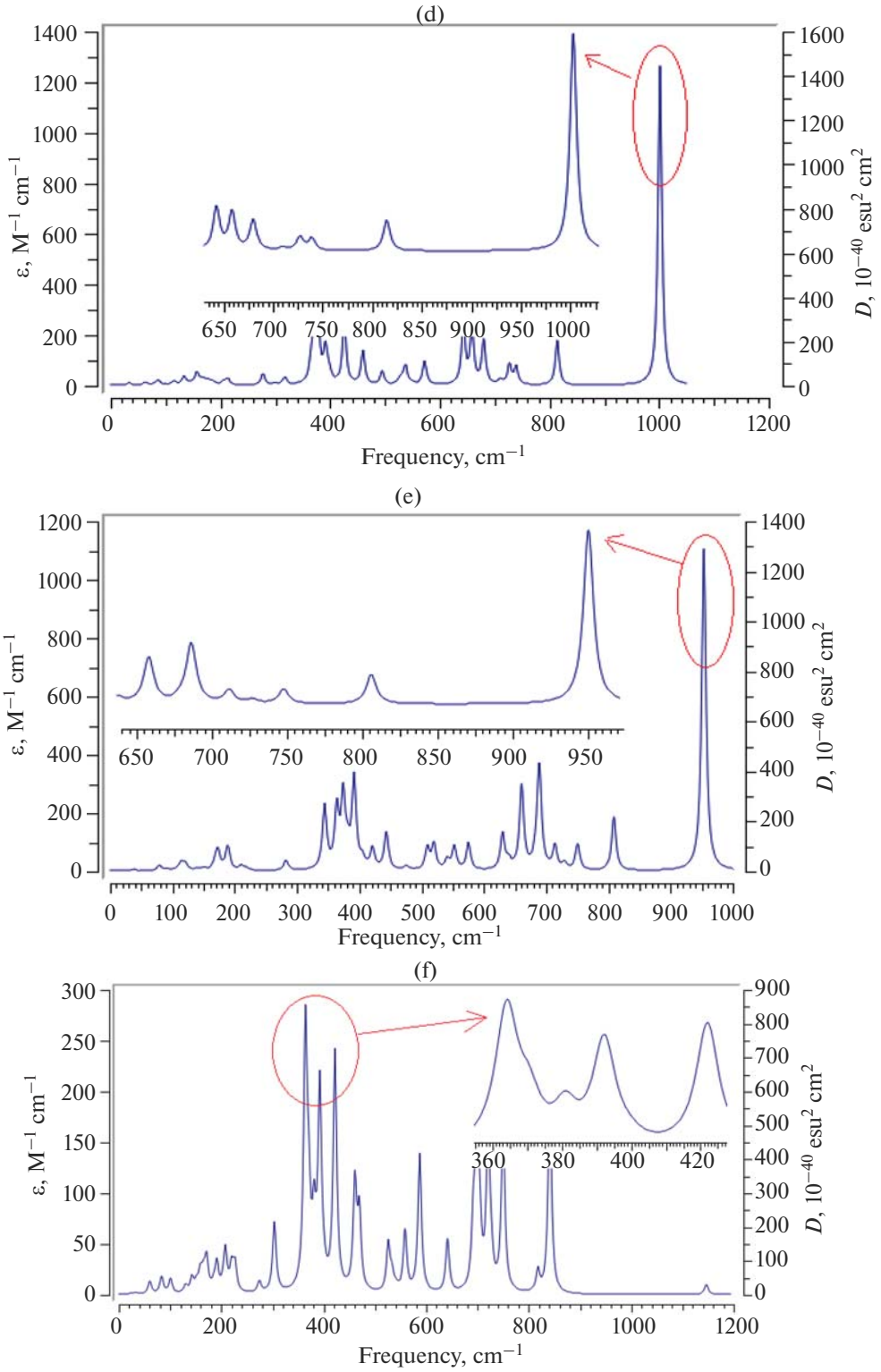

Fig. 7. (Contd.)

for certain high-frequency applications requiring solar cells for energy storage. The advantages of silver over indium gallium nitride include its higher electron and hole mobility, allowing silver doping devices to operate at higher frequencies than silicon and zinc doping devices.

Table 3. The thermodynamic characters of hetero clusters of GaN, InN, GaInN, GaInSiN, GaInZnN, and GaInAgN using CAM-B3LYP-D3/6-311+G(d,p) calculation

Compound	Dipole moment, D	$\Delta E^{\circ}_{ads} \times 10^{-3}$, kcal/mol	$\Delta H^{\circ}_{ads} \times 10^{-3}$, kcal/mol	$\Delta G^{\circ}_{ads} \times 10^{-3}$, kcal/mol	S°_{ads}, cal/K mol
GaN	4.7174	−319.300	−319.299	−319.344	149.170
InN	6.3277	−318.223	−318.222	−318.266	147.236
GaInN	4.6709	−318.743	−318.743	−318.788	151.994
GaInSiN	6.2553	−319.979	−319.978	−320.023	150.570
GaInZnN	5.9528	−358.610	−358.609	−358.655	151.603
GaInAgN	2.9453	−408.962	−408.962	−409.008	154.357

Table 3 through the thermodynamic specifications concluded that hetero clusters of GaN, InN, GaInN, GaInSiN, GaInZnN, and GaInAgN might be more efficient structure for energy storage in the solar cells.

Thermodynamic parameters of hetero clusters of GaN, InN, GaInN, GaInSiN, GaInZnN, and GaInAgN have been assigned through doping of ternary nanocluster of GaInN with Si, Zn and Ag towards formation hetero clusters (Table 3). The changes of Gibbs free energy versus dipole moment could detect the maximum efficiency of GaInAgN hetero cluster for energy storage in the solar cells through ΔG°_{ads} (Table 3).

The adsorption efficiency of GaN, InN, GaInN, GaInSiN, GaInZnN, and GaInAgN based on dipole moment has been evaluated by the ΔG°_{f}. The solar cells formed by GaN, InN, GaInN, GaInSiN, GaInZnN, and GaInAgN feature a hierarchical structure with the electron donor/acceptor layer sandwiched by anode and cathode, which raises the importance of controlling the molecular crystal orientation, domain size, and vertical distribution to facilitate the charge collection at electrodes. The doping obviously reduces indium atoms composition, the aggregation of In–In and induces the deep energy level. This greatly decreases the defects and improves the valence band potential of GaInN nanorods. In this paper, we have demonstrated that the ternary semiconductor of Indium Gallium Nitride structure can lead to a significant absorption enhancement in a broad spectral range of incident light in the presence of zinc and silver. A comparison between solar cells containing Si-, Zn-, or Ag-doped GaInN shows that the solar cells containing Zn or Ag structures show a more enhanced solar cell performance than the solar cells containing only the single GaInN structure. This efficient doping strategy not only bridges the gaps of heteroatom doped GaInN based photoelectrodes but also can provide deep insights into controlling the electronic structure for enhanced solar converting efficiency.

4. CONCLUSIONS

In summary, energy grabbing on the hetero clusters of GaN, InN, GaInN, GaInSiN, GaInZnN, GaInAgN as solar cells was investigated by first-principles calculations. We have provided a ternary semiconductor of Indium Gallium Nitride solar cell which is doped with silicon, zinc or silver. The geometrical parameters of doping atoms on the surface of GaInN through the absorption status and current charge density of the solar cells were studied. Moreover, the effect of a relative chemical shift between GaInN and doped hetero clusters of the solar cell was also investigated. Thermodynamic parameters have constructed a detailed molecular model for atom–atom interactions and a distribution of point charges which can be utilized to reproduce the polarity of the solid material and the adsorbing molecules. Energy storage with hetero clusters has described that the frame of the overcoming cluster is related to GaInAgN in the high amounts of frequency. This property makes GaInAgN potentially advantageous for certain high-frequency applications requiring solar cells for energy storage. The advantages of silver over indium gallium nitride include its higher electron and hole mobility, allowing silver doping devices to operate at higher frequencies than silicon and zinc doping devices. Thus, it should be explored its unique properties, such as its ability to increase energy storage which could lead to advancements in solar cells.

ACKNOWLEDGMENTS

In successfully completing this paper and its research, the author is grateful to Kastamonu University.

FUNDING

This work was supported by ongoing institutional funding. No additional grants to carry out or direct this particular research were obtained.

CONFLICT OF INTEREST

The author of this work declares that he has no conflicts of interest.

REFERENCES

1. Di Carlo, A., *Phys. Status Solidi A,* 2001, vol. 183, no. 1, p. 81. https://doi.org/10.1002/1521-396X(200101)183:1<81::AIDPSSA81>3.0.CO;2-N
2. Mollaamin, F. and Monajjemi, M., *Comput. Theor. Chem.,* 2024, vol. 1237, p. 114666. https://doi.org/10.1016/j.comptc.2024.114666
3. Sun J.D., Sun, Y.F., Wu, D.M., Cai, Y., Qin, H., and Zhang, B.S., *Appl. Phys. Lett.,* 2012, vol. 100, p. 013506. https://doi.org/10.1063/1.3673617
4. Mollaamin, F. and Monajjemi, M., *Russ. J. Phys. Chem. B,* 2024, vol. 18, p. 533. https://doi.org/10.1134/S199079312402012X
5. Amano, H., Sawaki, N., Akasaki, I., and Toyoda, Y., *Appl. Phys. Lett.,* 1986, vol. 48, no. 5, p. 353. https://doi.org/10.1063/1.96549
6. Amano, H., Kito, M., Hiramatsu, K., and Akasaki, I., *Jpn. J. Appl. Phys.,* 1989, vol. 28, no. 12, p. L2112. https://doi.org/10.1143/JJAP.28.L2112
7. Amano, H., Asahi, T., and Akasaki, I., *Jpn. J. Appl. Phys.,* 1990, vol. 29, no. 2, p. L205. https://doi.org/10.1143/JJAP.29.L205
8. Akasaki, I., Amano, H., Sota, S., Sakai, H., Tanaka, T., and Koike, M., *Jpn. J. Appl. Phys.,* 1995, vol. 34, no. 11B, p. L1517. https://doi.org/10.7567/JJAP.34.L1517
9. Kodama, M., Sugimoto, M., Hayashi, E., Soejima, N., Ishiguro, O., Kanechika, M., Itoh, K., Ueda, H., Uesugi, T., and Kachi, T., *Appl. Phys. Express,* 2008, vol. 1, p. 021104. https://doi.org/10.1143/APEX.1.021104
10. Wraback, M., Shen, H., Carrano, J.C., Collins, C.J., Campbell, J.C., Dupuis, R.D., Schurman, M.J., Ferguson, I.T., *Appl. Phys. Lett.,* 2000, vol. 76, no. 9, p. 1155. https://doi.org/10.1063/1.125968
11. Wu, J., Walukiewicz, W., Yu, K.M., et al., *J. Appl. Phys.,* 2003, vol. 94, p. 6477.
12. Wu, J., Walukiewicz, W., Yu, K., et al., *Appl. Phys. Lett.,* 2002, vol. 80, p. 4741.
13. Singh, R., Doppalapudi, D., Moustakas, T.D., and Romano, L.T., *Appl. Phys. Lett.,* 1997, vol. 70, p. 1089.
14. Lien, D.H., Hsiao, Y.H., Yang, S.G., et al., *Nano Energy,* 2015, vol. 11, p. 104.
15. Kuwahara, Y., Fujii, T., Fujiyama, Y., et al., *Appl. Phys. Express,* 2010, vol. 3, p. 111001.
16. Young, N.G., Farrell, R.M., Hu, Y.L., et al., *Appl. Phys. Lett.,* 2013, vol. 103, p. 1739031.
17. Neufeld, C.J., Cruz, S.C., Farrell, R.M., et al., *Appl Phys Lett.,* 2011, vol. 98, p. 2435071.
18. Okoampa Boadu, E., Van Wellington, E., and Abu, Y., *Materials,* 2024, vol. 6, no. 1, p. 5. https://doi.org/10.33263/Materials61.005
19. Wang, K.X., Yu, Z., Liu, V., Cui, Y., and Fan, S., *Nano Lett.,* 2012, vol. 12, p. 1616.
20. Meng, X., Drouard, E., Gomard, G., Peretti, R., Fave, A., and Seassal, C., *Opt. Express,* 2012, vol. 20, p. A560.
21. Abass, A., Le, K.Q., Alu, A., Burgelman, M., and Maes, B., *Phys. Rev. B,* 2012, vol. 85, p. 1154491.
22. Chriki, R., Yanai, A., Shappir, J., and Levy, U., *Opt. Express,* 2013, vol. 21, p. A382.
23. Hsu, W.C., Tong, J.K., Branham, M.S., et al., *Opt. Commun.,* 2016, vol. 377, p. 52.
24. Isabella, O., Vismara, R., Ingenito, A., Rezaei, N., and Zeman, M., *Opt. Express,* 2016, vol. 24, p. A708.
25. Lin, J., Yu, Y., Xu, Z., Gao, F., Zhang, Z., Zeng, F., Wang, W., and Li, G., *J. Power Sources,* 2020, vol. 450, p. 227578. https://doi.org/10.1016/j.jpowsour.2019.227578
26. Kumawat, U.K., Kumar, K., Bhardwaj P., and Dhawan, A., *Energy Sci. Eng.,* 2019, vol. 7, no. 6, p. 2469. https://doi.org/10.1002/ese3.436
27. Mollaamin, F. and Monajjemi, M., *Mol. Simul.,* 2023, vol. 49, p. 365. https://doi.org/10.1080/08927022.2022.2159996
28. Zadeh, M.A.A., Lari, H., Kharghanian, L., et al., *J. Comput. Theor. Nanosci.,* 2015, vol. 12, p. 4358. https://doi.org/10.1166/jctn.2015.4366
29. Mollaamin, F. and Monajjemi, M., *J. Cluster Sci.,* 2023, vol. 34, p. 2901. https://doi.org/org/10.1007/s10876-023-02436-5.
30. Sarasia, E.M., Afsharnezhad, S., Honarparvar, B., et al., *Phys. Chem. Liq.,* 2011, vol. 49, p. 561. https://doi.org/10.1080/00319101003698992
31. Mollaamin, F., Shahriari, S., Monajjemi, M., et al., *J. Cluster Sci.,* 2023, vol. 34, p. 1547. https://doi.org/10.1007/s10876-022-02335-1
32. Tahan, A., Mollaamin, F., and Monajjemi, M., *Russ. J. Phys. Chem. A,* 2009, vol. 83, p. 587. https://doi.org/10.1134/S003602440904013X
33. Mollaamin, F. and Monajjemi, M., *J. Mol. Model.,* 2023, vol. 29, p. 119. https://doi.org/10.1007/s00894-023-05526-3
34. Khalili Hadad, B., Mollaamin, F., and Monajjemi, M., *Russ. Chem. Bull.,* 2011, vol. 60, p. 238. https://doi.org/10.1007/s11172-011-0039-5
35. Mollaamin, F. and Monajjemi, M., *J. Mol. Model.,* 2023, vol. 29, p. 170. https://doi.org/10.1007/s00894-023-05567-8
36. Monajjemi, M., Baie, M.T., and Mollaamin, F., *Russ. Chem. Bull.,* 2010, vol. 59, p. 886. https://doi.org/10.1007/s11172-010-0181-5
37. Mollaamin, F., *Russ. J. Phys. Chem. B,* 2024, vol. 18, p. 805. https://doi.org/10.1134/S1990793124700131
38. Mollaamin, F. and Monajjemi, M., *Int. J. Quantum Chem.,* 2024, vol. 124, p. e27348. https://doi.org/10.1002/qua.27348
39. Mollaamin, F. and Monajjemi, M., *Mol. Simul.,* 2023, vol. 49, no. 4, p. 365. https://doi.org/10.1080/08927022.2022.2159996
40. Vosko, S.H., Wilk, L., and Nusair, M., *Can. J. Phys.,* 1980, vol. 58, no. 8, p. 1200. https://doi.org/10.1139/p80-159

41. Frisch, M.J., Trucks, G.W., Schlegel, H.B., Scuseria, G.E., Robb, M.A., et al., *Gaussian 16, Revision C.01,* Wallingford, CT: Gaussian, Inc., 2016.

42. Dennington, R., Keith, T.A., and Millam, J.M., *GaussView, Ver. 6.06.16,* Shawnee Mission, KS: Semichem Inc., 2016.

43. Xu, Z., Qin, C., Yu, Y., Jiang, G., and Zhao, L., *AIP Adv.,* 2024, vol. 14, p. 055114. https://doi.org/10.1063/5.0208082

44. O'Boyle, N.M., Tenderholt, A.L., and Langner, K.M., *J. Comput. Chem.,* 2008, vol. 29, p. 839.

45. Murray, J.S. and Politzer, P., *Wiley Interdiscip. Rev.: Comput. Mol. Sci.,* 2011, vol. 1, no. 2, p. 153. https://doi.org/10.1002/wcms.19

46. Lu, T. and Chen, F., *J. Comput. Chem.,* 2012, vol. 33, p. 580. https://doi.org/10.1002/jcc.22885

47. Lu, T., *J. Chem. Phys.,* 2024, vol. 161, p. 082503. https://doi.org/10.1063/5.0216272

48. Trontelj, Z., Pirnat, J., Jazbinšek, V., Lužnik, J., Srčič, S., Lavrič, Z., Beguš, S., Apih, T., Žagar, V., and Seliger, J., *Crystals,* 2020, vol. 10, p. 450. https://doi.org/10.3390/cryst10060450

49. Sciotto, R., Ruiz Alvarado, I.A., and Schmidt, W.G., *Surfaces,* 2024, vol. 7, p. 79. https://doi.org/10.3390/surfaces7010006

50. Luo, J., Wang, C., Wang, Z., Guo, Q., Yang, J., Rui Zhou, R., Matano, K., Oguchi, T., and Ren, Z., *Chin. Phys. B,* 2020, vol. 29, p. 067402. https://doi.org/10.1088/1674-1056/ab892d

51. Young, H.A. and Freedman, R.D., *Sears and Zemansky's University Physics with Modern Physics,* Boston: Addison-Wesley, 2012, p. 754.

52. Bakhshi, K., Mollaamin, F., and Monajjemi, M., *J. Comput. Theor. Nanosci.,* 2011, vol. 8, p. 763. https://doi.org/10.1166/jctn.2011.1750